

A Parallel Queue Structure for Active Queue Management

Jia-Shiang Jou, Xiaobo Tan and John S. Baras
 Department of Electrical and Computer Engineering
 and Institute for Systems Research
 University of Maryland, College Park, MD 20742 USA
 {jsjou, xbtan, baras}@isr.umd.edu

Abstract—Performance of the Adaptive RED scheme is susceptible to bursty web traffic. A parallel queue structure was proposed earlier to address this problem, where real time connections (such as web and UDP) and non-real time connections (such as FTP) are served in two different queues with drop-tail and Adaptive RED policies, respectively. In this paper a modified Adaptive RED scheme is proposed for the second queue to improve the goodput of non-real time connections. In this scheme the queue length thresholds for the Adaptive RED are dynamically determined by the average dropping probability. Simulation shows that the packet dropping probability of the Adaptive RED queue stays within a desired small region. The stability of the queue length variation under this policy is proved under mild conditions.

Index Terms—Adaptive RED, Active Queue Management, Scheduling, Stability.

I. INTRODUCTION

The basic idea of RED (Random Early Detection) is to randomly drop packets to prevent buffer overflow and the global synchronization problem [1]. The dropping probability is a non-decreasing function of the queue length as shown in Figure 1. A TCP connection with a higher flow rate has a better chance to get packets dropped and reduces its rate more rapidly. By dropping packets actively, RED keeps the queue length within a desired region. However, some simulation and analysis results [2] [3] [4] have demonstrated that the performance of RED is very sensitive to parameter settings. Based on the original idea of RED, there have been some modifications such as Stabilized RED (SRED) [5], Flow RED (FRED) [6], Weighted RED [7], Random Early Marking (REM) [8], BLUE [9] and Adaptive RED [10] [11]. The Adaptive RED scheme dynamically updates the maximum dropping probability P_{max} according to the exponentially weighted moving average (EWMA) of the queue length and the overflow/underflow events of queue length. In particular P_{max} is increased if the average queue length is greater than $maxth$ and decreased if average queue length is less than $minth$. The average queue length can thus be kept in the region $(minth, maxth)$. This adaptive scheme makes itself more robust with respect to the congestion level.

The Adaptive RED policy provides good rate control for TCP connections operating in the congestion avoidance phase.

Research partially supported by DARPA through SPAWAR, San Diego under contract No. N66001-00-C-8063.

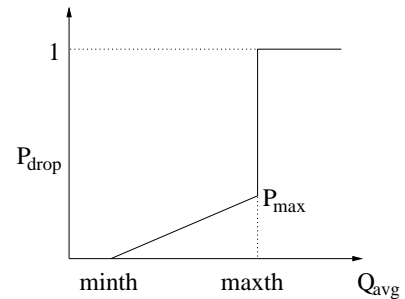


Fig. 1. The dropping probability function of the original RED.

However, a great portion of Internet traffic is web and UDP traffic. Since most web connections involve transfer of several small files, these connections have a short life and are mostly operated in the TCP slow start phase with a small congestion window. Dropping web packets by RED in this phase is not an effective way to control the traffic rate and alleviate the congestion at the bottleneck router. Furthermore, from the viewpoint of a web user, one or several packet losses in the slow start phase would lead to extra delay for retransmission or even TCP timeout. It would also force TCP to enter the congestion avoidance phase prematurely with a small congestion window and result in a low throughput. This delay and low throughput would severely degrade the performance of delivering short messages such as web pages, and web browsers would experience long waiting times even with a high speed network as shown in Figure 2. To address these problems, we propose a parallel queue structure for active queue management at the router in [12]. In this structure short-life and delay sensitive traffic such as web is bypassed to a separate queue as shown in Figure 3, and the Adaptive RED queue is only responsible for handling delay insensitive applications such as FTP.

The original Adaptive RED dynamically changes the maximum dropping probability P_{max} to keep the queue length within the thresholds. However, for non-real time applications, high goodput (low packet dropping rate) is more important than short packet delay. Hence in this paper we explore a modified Adaptive RED policy for non-real time applications at the second queue in which the queue length thresholds are dynamically adjusted to maintain the dropping probability of Adaptive RED algorithm in a desired range. Simulation results

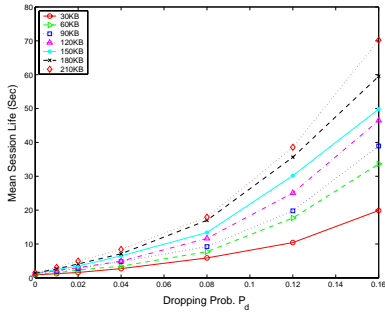


Fig. 2. TCP/Reno mean delivery delay of small file *v.s.* dropping probability P_d with file sizes 30, 60, ..., 210Kbytes, bandwidth 3Mbps and round-trip time 128ms.

show that high link utilization is achieved while the packet dropping probability for the Adaptive RED queue stays in a desired (small) region. This scheme allows one to control the rates of non-real time connections using queuing delay (not a problem for such connections) instead of the dropping probability. A question that arises naturally is whether the queue length variation under the modified Adaptive RED is stable. We shall provide an affirmative answer to this question through analysis of queue length dynamics.

The remainder of the paper is organized as follows. In Section II the parallel queue structure is briefly reviewed. The Adaptive RED scheme with dynamic thresholds is described in Section III. Section IV contains the stability analysis of the queue length dynamics. Finally, we conclude in Section V.

II. A PARALLEL QUEUES STRUCTURE

In this section we briefly introduce the parallel queue structure proposed in [12]. The first queue serves UDP packets and short-life real-time traffic such as web traffic. Since dropping these UDP and web packets cannot effectively alleviate the congestion level, it would be good to keep them in the queue unless the total buffer (shared with the other queue) has overflowed. Hence, the queuing policy of this queue is chosen to be drop-tail to minimize the packet loss rate. In order to have a short file delivery delay for UDP and web connections, the service rate $C_1(t)$ is changed dynamically according to its instant queue length $q_1(t)$ at time t .

The second queue serves long-life TCP connections such as FTP with large file sizes, where the Adaptive RED is used. Figure 3 shows the RED+Tail parallel queue structure in the router. In order to allocate bandwidth dynamically to both queues and assign a desired region of queue length for the Adaptive RED queue, we define the maximum thresholds $maxth_i$ and minimum thresholds $minth_i$ for $i = 1, 2$. The service rates $C_1(t)$ and $C_2(t)$ are given by the following algorithm:

- if $q_1(t) = 0$, then $C_1(t) := 0$.
- if $0 < q_1(t) < minth_1$, then $C_1(t) := C_{1min}$.
- if $minth_1 \leq q_1(t)$, then $C_1(t) := \min(C_{\frac{q_1(t)}{maxth_1}}, C_{1max})$.
- $C_2(t) := C - C_1(t)$,

where C is the link bandwidth. The constant C_{1max} preserves the minimum available bandwidth $C - C_{1max}$ for the RED

queue to prevent FTP connections from timeout. The thresholds $maxth_2$ and $minth_2$ fixed in the original Adaptive RED, are used to regulate the maximum dropping probability, i.e., the maximum dropping probability P_{max} is adjusted when the average queue length is outside $[minth_2, maxth_2]$.

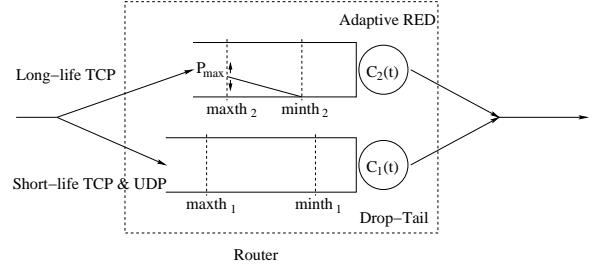


Fig. 3. The parallel queue structure for active queue management (Fixed Thresholds) .

Although the available bandwidth of the Adaptive RED queue is shared with the drop-tail queue, $q_2(t)$ stays in a desired region [12]. With this RED+Tail parallel queue structure, we can keep the benefits of Adaptive RED such as high (100%) link utilization. Furthermore, the packet loss rate of UDP and web connections is greatly reduced by the drop-tail policy and a shared buffer. The packet loss rate of long-life TCP traffic is also reduced due to a more stable queue length in the Adaptive RED queue [12]. Figure 4 compares the small web file delivery time under different buffer management schemes such as Drop-Tail, Adaptive RED and RED+Tail.

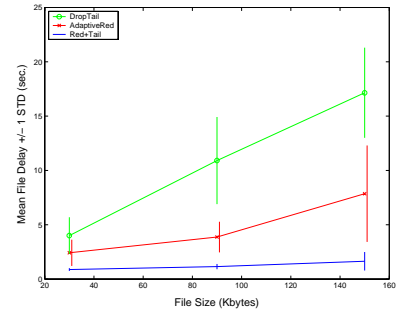


Fig. 4. Small file delivery delay: mean and standard deviation.

III. ADAPTIVE RED WITH DYNAMIC THRESHOLDS

The original Adaptive RED dynamically adjusts the P_{max} (or equivalently, the slope of dropping function) to control the flow rates of TCP connections and keep the average queue length in a desired region. However, for those applications with large file sizes, the goodput is more important than the packet delay. The packet loss rate is a key factor in determining the TCP congestion window size and goodput. Since the minimum and maximum thresholds of the Adaptive RED scheme are fixed, the dropping probability of Adaptive RED could be very high when a congestion happens. This high dropping probability causes frequent re-transmissions, small average congestion window size and low goodput. In other words, the congestion in bottleneck router causes another bottleneck at the TCP sender end. Considering that the Adaptive RED

queue is designed for serving time insensitive connections, we propose to control the TCP flow rate by adjusting its queuing delay instead of dropping packets.

To maintain a low packet loss rate (and a large average congestion window size at the TCP sender), the following modified Adaptive RED scheme for the Adaptive RED queue is proposed, where $minth_2$ and $maxth_2$ are dynamically adjusted while $D=maxth_2 - minth_2$ is maintained constant:

- Pick $0 < \gamma < 1$ ($\gamma=0.05$ in this paper).
- If $\bar{P}_d > P_U$, then $minth_2 := minth_2(1 + \gamma)$, $maxth_2 := minth_2 + D$.
- If $\bar{P}_d < P_L$, then $minth_2 := minth_2(1 - \gamma)$, $maxth_2 := minth_2 + D$,

where \bar{P}_d is the average dropping probability obtained by the EWMA algorithm and (P_L, P_U) is the desired region of dropping probability. Note that if we set $P_U < P_{max}$, the floating thresholds do not change the current slope of dropping probability function dramatically since the distance between the thresholds is fixed.

The rationale behind the above scheme is that, by increasing the thresholds (when $\bar{P}_d > P_U$), the queuing delay is increased and the flow rates are reduced. Since the average TCP throughput [13] is proportional to $\frac{1}{RTT\sqrt{\bar{P}_d}}$, we achieve the same throughput without raising the packet loss rate. Figures 5 and 6 obtained in ns2 simulation compare the Adaptive RED schemes with fixed and dynamic thresholds respectively. There are 20 persistent FTP servers sharing a 6Mbps bottleneck link. Another 20 FTP servers arrive at time 100s and leave at time 300s. It can be seen that the fixed threshold scheme has a small queue length variation and a large dropping probability (0.05). In contrast, the dynamic threshold scheme has a much lower average dropping probability (0.014 with $P_L=0.010$, $P_U=0.020$), but a higher packet delay. Note that both schemes achieve 100% link utilization so that each FTP connection has the same throughput. However, with a much lower packet loss rate, the scheme with dynamic thresholds achieves a higher goodput. This scheme provides a trade-off between packet loss and queuing delay in an Adaptive RED queue.

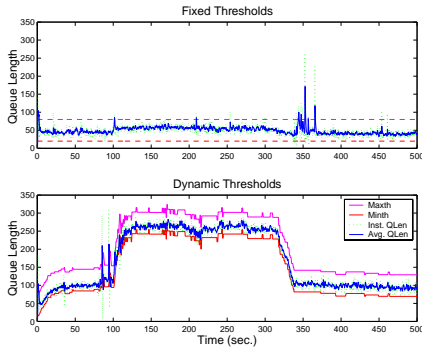


Fig. 5. Average queue length with fixed and dynamic thresholds: 20 FTP starting at $t=0$, and another 20 FTP starting at $t=100s$ and leaving at $t=300s$, $C=6Mbps$, $d_k=64ms$.

We also implemented the Adaptive RED with dynamic thresholds in the parallel queue structure, and compared with the case where the fixed threshold Adaptive RED was used. The network in our ns2 experiment has a simple dumbbell

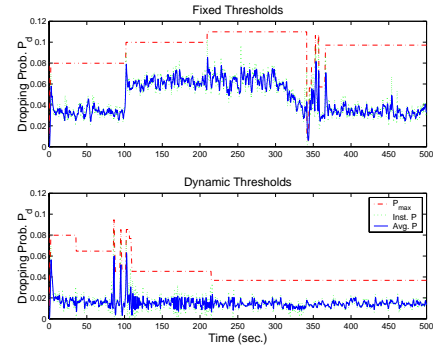


Fig. 6. Dropping probability with fixed and dynamic thresholds: 20 FTP starting at $t=0$, and another FTP 20 starting at $t=100s$ and leaving at $t=300s$, $C=6Mbps$, $d_k=64ms$ (Inst. P: instantaneous dropping probability; Avg. P: EWMA average of Inst. P).

topology with the bottleneck link bandwidth $C=3.0Mbps$. One side of the bottleneck consists of 800 web clients. Each client sends a web request and has a think time of *Exponential* distribution with mean 50s after the end of each session. The other side contains 800 web servers, running HTTP 1.1 protocol and having a *Pareto* file size distribution with parameters ($K_p=2.3Kbytes$, $\alpha=1.3$) (mean 10Kbytes). The round-trip propagation delay of HTTP connections is uniformly distributed in (16, 240)ms. Note that the mean rate of the aggregate web traffic is around 1.2Mbps. There is one CBR traffic source which periodically generates a 1Kbytes UDP packet every 50ms. Besides the short web connections and UDP traffic, there are 10 persistent FTP connections sharing the bottleneck link with round-trip propagation delay of 64ms. Web and CBR traffic go to the first (drop-tail) queue and FTP traffic goes to the second (Adaptive RED) queue at the bottleneck router. Table I compares the performance of each type of connection, and the results are consistent with Figure 5 and Figure 6. We also note that in the dynamic threshold scheme the packet loss rate of q_1 is slightly higher than that in the fixed threshold scheme. This is due to the longer average length of the RED queue (and thus smaller buffer for q_1 since both queues share the same physical memory) when the dynamic threshold scheme is used. This situation can be improved by increasing the total buffer size despite that this approach is general useless or even harmful in a single RED queue or a single drop-tail queue.

TABLE I
PERFORMANCE METRICS: RED+TAIL WITH FIXED AND DYNAMIC THRESHOLD SCHEMES RESPECTIVELY

Policy	Loss %	Delay Sec.	Rate KB/s
Fix. Thres.:FTP(q_2)	2.747	0.184	209.465
Fix. Thres.:WEB(q_1)	1.278	0.114	144.455
Fix. Thres.:CBR(q_1)	0.300	0.109	19.867
Dyn. Thres.:FTP(q_2)	0.899	0.318	209.455
Dyn. Thres.:WEB(q_1)	2.306	0.093	144.505
Dyn. Thres.:CBR(q_1)	0.519	0.091	19.827

IV. STABILITY ANALYSIS OF THE QUEUE LENGTH DYNAMICS

In Section III we proposed the modified Adaptive RED scheme with dynamic thresholds in the parallel queue structure for controlling the flow rate of non-real time applications. The maximum threshold $maxth_2$ and minimum threshold $minth_2$ are changed dynamically to keep the packet dropping probability P_d within a desired small region (P_L, P_U) at the cost of packet delay variation. In this section we analyze issues related to the stability of this queue. To simplify the analysis, it is assumed that the dropping probability P_d of the Adaptive RED at the bottleneck router is fixed so that the average flow rate of each TCP connection can be approximated by a simple function of its round-trip time (RTT). Note that this assumption is not very restrictive considering that the interval (P_L, P_U) is small.

Consider N persistent TCP flows. Define T_k^n as the average flow rate of the k^{th} TCP connection during time slot n . Let d'_k be the link round-trip propagation delay of connection k . At the beginning of time slot n , the k^{th} connection sees a round-trip time R_k^n which is equal to the sum of link propagation delay and the average queuing delay in the forward direction q^n/C and in the backward direction q_b^n/C :

$$R_k^n = d'_k + \frac{q^n}{C} + \frac{q_b^n}{C}, \quad (1)$$

where C is the link bandwidth, q^n and q_b^n are the forward queue length and the backward queue length at the beginning of time slot n , respectively. We assume that congestion only happens in the forward direction, and the queuing delay q_b^n/C in the backward direction is a constant. Hence we can write $R_k^n = d_k + q^n/C$ with $d_k = d'_k + q_b^n/C$.

Based on the assumption of fixed dropping probability at the router, each TCP connection experiences a fixed packet loss rate P_d . As a result, the corresponding average congestion window size is assumed to be a constant \bar{W} , and the average flow rate T_k^n of the k^{th} TCP connection at slot n is

$$T_k^n = \frac{\bar{W}}{R_k^n} + E_k^n \quad (2)$$

where E_k^n is a white Gaussian process with zero mean and variance σ^2 modeling the flow rate perturbation of the k^{th} connection at slot n .

Given the arrival rate of each TCP connection, the dynamics of queue length q^n follows the *Lindley* equation:

$$q^{n+1} = \min\{B, \max[0, q^n + (\sum_{k=1}^N T_k^n - C)S]\}, \quad (3)$$

where B is the buffer size and S is the duration of one time slot. Since the queue length of Adaptive RED is mostly operated in a region far from the boundary, we first ignore the *max* and *min* operations in (3) and have a simplified nonlinear dynamic system:

$$q^{n+1} = f(q^n) + \xi^n, \quad (4)$$

where

$$f(q^n) \triangleq q^n + S\left\{\left(\sum_{k=1}^N \frac{\bar{W}C}{q^n + d_k C}\right) - C\right\}, \quad (5)$$

and

$$\xi^n \triangleq S \sum_{k=1}^N E_k^n. \quad (6)$$

To avoid the trivial case $q \equiv 0$, we assume that the sum of possible peak rates of all connections is greater than the link bandwidth at the bottleneck router:

$$\sum_{k=1}^N \frac{\bar{W}}{d_k} \geq C. \quad (7)$$

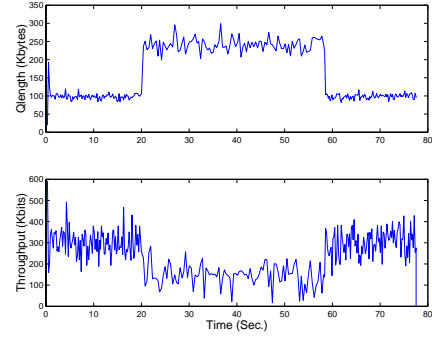


Fig. 7. Queue length and TCP throughput (of a single connection) with $C=6$ Mbps, $d_k=64$ ms, $\bar{W}=6.02 \times 10^4$ bits. Compare with simulation in Fig.5.

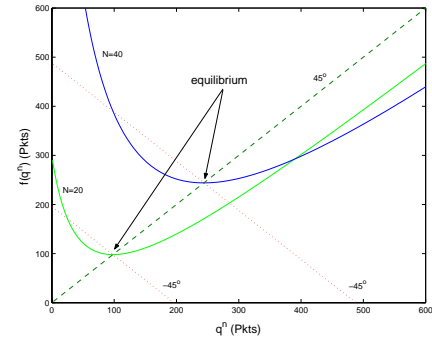


Fig. 8. Mapping functions and equilibrium points when $N=20, 40$ with $S=RTT$.

Figure 7 shows the queue length dynamics (and the throughput of a persistent TCP connection) based on the model (4), where the flow rate deviations $\sigma = 77021, 128490$ (bits/s) for $N=20, 40$ are measured from the simulation in Section III, respectively. For both $N = 20$ and $N = 40$, Figure 7 shows consistent steady state behavior with simulation results in Figure 5. The mapping $f(\cdot)$ is plotted in Figure 8 for $N = 20$ and $N = 40$.

We first analyze the stability of the equilibrium of the model (4) when there is no flow disturbance, *i.e.*, $E_k^n = 0$. An equilibrium q_e of $q^{n+1} = f(q^n)$ should satisfy

$$\sum_{k=1}^N \frac{\bar{W}}{d_k + q^n/C} = C. \quad (8)$$

Since $\sum_{k=1}^N \frac{\bar{W}}{d_k} \geq C$ by assumption, (8) has a unique solution q_e in $[0, \infty)$. q_e is located at the intersection of the graph of f with the 45° line (see Figure 8).

It is well known that q_e is locally asymptotically stable if $|f'(q_e)| < 1$. In the following we give conditions for q_e to be globally asymptotically stable.

Proposition 4.1: If the rate update interval S satisfies

$$S < \frac{2C}{\bar{W}(\sum_{k=1}^N d_k^{-2})}, \quad (9)$$

the equilibrium q_e is globally asymptotically stable. Furthermore, $|q^n - q_e| < \rho^n |q^0 - q_e|$ for some $\rho \in (0, 1)$ dependent on q^0 .

Proof: First we observe that the function f is convex since

$$f''(q) = \sum_{k=1}^N \frac{2S\bar{W}C}{(q + d_k C)^3} > 0, \quad \forall q \in [0, \infty). \quad (10)$$

For any B_0 such that $B_0 > q_e$ and

$$B_0 \geq f(0) = \left(\sum_{k=1}^N \frac{\bar{W}}{d_k} - C \right) S, \quad (11)$$

one can verify that f maps $[0, B_0]$ to $[0, B_0]$ due to convexity of f and

$$f'(q) = 1 - S \sum_{k=1}^N \frac{\bar{W}C}{(q + d_k C)^2} < 1, \quad \forall q \in [0, \infty). \quad (12)$$

When restricted to $[0, B_0]$, $f'(q) \leq \rho_1$ with $\rho_1 \in (0, 1)$. If (9) is satisfied, $f'(q) > -1$, $\forall q \in [0, \infty]$, and $f'(q) \geq -\rho_2$, $\forall q \in [0, B_0]$, with $\rho_2 \in (0, 1)$.

Hence $|f'(q)| \leq \rho \triangleq \max(\rho_1, \rho_2) < 1 \forall q \in [0, B_0]$, which implies that f is a contraction mapping on $[0, B_0]$. By the Contraction Mapping Principle [14],

$$|q^n - q_e| < \rho^n |q^0 - q_e|, \quad \text{if } q^0 \in [0, B_0]. \quad (13)$$

Since B_0 can be arbitrarily large (as long as $B_0 < \infty$), q_e is globally asymptotically stable. Note that the contraction constant ρ depends on B_0 and thus on q^0 . \square

From Proposition 4.1, when rate update is frequent enough, the equilibrium will be asymptotically stable (the equilibrium itself does not depend on S). Another sufficient condition for asymptotic stability is the following:

Proposition 4.2: If $f'(q_e) \geq 0$, then q_e is a globally asymptotically stable.

Proof: As shown in the proof of Proposition 4.1, f is convex. If $f'(q_e) \geq 0$, graphical analysis reveals that

$$|q^{n+1} - q_e| \leq |q^n - q_e|,$$

where the equality holds if and only if $q^n = q_e$. The claim thus follows. \square

For the homogeneous case $d_k = d$, we have $q_e = N\bar{W} - dC$. And the condition $f'(q_e) \geq 0$ is equivalent to $S \leq \frac{N\bar{W}}{C} = q_e/C + d$. In other words, q_e is asymptotically stable if the rate update interval S is no larger than the round-trip time (RTT). Figure 9 shows the mapping f and the equilibrium q_e for different S . Figure 10 shows the queue length dynamics

for $S=RTT$ and $2RTT$, respectively. We can see that in the case $S=RTT$, the queue length stays around q_e with small variation, while in the case $S=2RTT$, the queue length dynamics is much more chaotic.

For the heterogeneous case, a sufficient condition $S \leq \left(\frac{C}{\bar{W}} - \frac{N(N-1)}{(q_e + C \min_k d_k)^2} \right)^{-1}$ for stability can be derived.

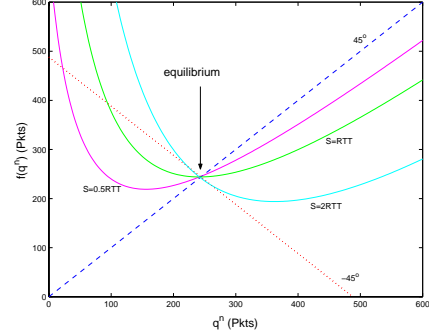


Fig. 9. Mapping function and equilibrium point when $N=40$ with $S=0.5RTT$, $1RTT$ and $2RTT$.

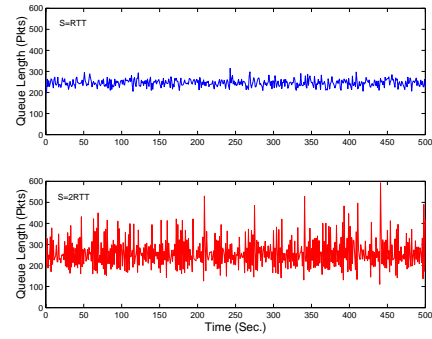


Fig. 10. Queue length with $N=40$, $S=RTT$ and $2RTT$.

Next we consider the *Lindley* equation with random perturbation $\xi^n = S \sum_{k=1}^N E_k^n$:

$$q^{n+1} \triangleq g(q^n, \xi^n) = \min\{B, \max[0, f(q^n) + \xi^n]\} \quad (14)$$

Note that since $\{E_k^n\}$ is white and stationary, so is $\{\xi^n\}$. It turns out that stability of the equilibrium of the deterministic system $q^{n+1} = f(q^n)$ is closely related to stochastic stability of the system (14).

Proposition 4.3: The stochastic system (14) admits an invariant probability measure μ^* for the queue length q^n . Furthermore, if the condition (9) on Proposition 4.1 is satisfied, this system is weakly asymptotically stable, *i.e.*, the queue length distribution μ^n for q^n converges to μ^* weakly.

Sketch of Proof. Since f is continuous and $\{\xi^n\}$ is identically and independently distributed, the system (14) is a regular stochastic dynamic system [15].

Since $[0, B]$ is compact, the system admits an invariant probability measure μ^* by the *Krylov-Bogolubov* Theorem [15]. When condition (9) is satisfied, g is a contraction mapping with respect to its first argument, *i.e.*,

$$|g(x, \xi) - g(y, \xi)| < \rho |x - y|, \quad \forall x, y \in [0, B], \forall \xi, \quad (15)$$

where $\rho \in (0, 1)$. Hence the system is weakly asymptotically stable by Theorem 12.6.1 of [15]. \square

The invariant probability measure μ^* has probability masses at $q = 0$ and $q = B$, and has probability density on $(0, B)$. An approximation to μ^* can be obtained by numerically advancing the probability distribution μ^n for the queue length q^n . We have discretized the queue length and consequently obtained a Markov chain for the dynamics of the queue length distribution.

Let the packet size have a fixed length L (bits), $z^n := \text{ceil}(q^n/L)$ be the number of packets in the queue at time n and $\pi^n = [Pr(z^n = 0), \dots, Pr(z^n = B)]$ denote the corresponding probability vector. Denote by T the state transition matrix of the Markov Chain, where $T(i, j) = Pr[z^{n+1} = j | z^n = i] = Pr[j \leq (\min\{B, \max\{0, f(iL) + \xi\})/L < (j + 1)]$. We have

$$\pi^{n+1} = \pi^n T, \quad (16)$$

$$\pi^* = \pi^* T, \quad (17)$$

where $\pi^* = \lim_{n \rightarrow \infty} \pi^n$ is the steady state distribution.

On the other hand, when the buffer size B is far greater than the equilibrium queue length and the perturbation magnitude is small, the transformation $g(q, \xi)$ can be linearized around the equilibrium point q_e . Let $Q^n \triangleq q^n - q_e$. Then

$$Q^{n+1} \triangleq f'(q_e)Q^n + \xi^n. \quad (18)$$

Since $\{\xi^n\}$ is white Gaussian process with zero mean and variance $NS\sigma^2$, $\{Q^n\}$ will be a Gaussian process with zero mean and normalized variance

$$\text{Var}[Q^n/S] = \frac{N\sigma^2}{1 - |f'(q_e)|^2}. \quad (19)$$

From (19) the normalized queue length variation will be minimal if $f'(q_e) = 0$, which corresponds to $S = RTT$ for the homogeneous case.

Figure 11 shows the queue length distributions obtained through empirical estimation from ns2 simulation, numerical computation based on (16), and linear approximation based on (19), respectively. Three distributions agree well, which verifies that our nonlinear model (14) captures the queue length dynamics under the Adaptive RED scheme with dynamic thresholds.

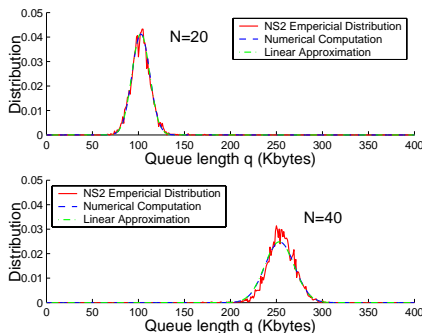


Fig. 11. Steady state queue length distributions for $N=20$ and 40 , $S=RTT$.

V. CONCLUSIONS

In this paper we have first reviewed the parallel queue structure for active queue management. This structure offers more degrees of freedom to its flexibility in accommodating variants of the Adaptive RED scheme. We have explored a modified Adaptive RED scheme with sliding queue length thresholds. This scheme is able to maintain the dropping probability within a small interval and improve the goodput of non-real time connections. The queue length variation under this policy has been analyzed and conditions for its stability have been given. The dynamic threshold Adaptive RED might also be useful for achieving throughput fairness among multiple RED queues.

REFERENCES

- [1] S. Floyd and V. Jacobson, "Random early detection gateways for congestion avoidance," *IEEE/ACM Transactions on Networking*, vol. 1, no. 4, pp. 397–413, 1993.
- [2] M. Christiansen, K. Jaffay, D. Ott, and F.D. Smith, "Tuning RED for web traffic," in *Proceedings of SIGCOMM*, 2000, pp. 139–150.
- [3] V. Misra, W. Gong, and D. F. Towsley, "Fluid-based analysis of a network of AQM routers supporting TCP flows with an application to RED," in *Proceedings of SIGCOMM*, 2000, pp. 151–160.
- [4] P. Ranjan, E. Abed, and R. La, "Nonlinear instabilities in TCP-RED," in *Proceedings of INFOCOM*, 2002, pp. 249–258.
- [5] T. J. Ott, T. V. Lakshman, and L. H. Wong, "SRED: Stabilized RED," in *Proceedings of INFOCOM 99*, 1999, pp. 1346–1355.
- [6] D. Lin and R. Morris, "Dynamics of random early detection," in *Proceedings of SIGCOMM*, 1997, pp. 127–137.
- [7] D. Clark and W. Feng, "Explicit allocation of best-effort packet delivery service," *IEEE/ACM Transactions on Networking*, vol. 6, no. 4, pp. 362–373, Aug. 1998.
- [8] S. Athuraliya, S. Low, V. Li, and Q. Yin, "REM: Active queue management," *IEEE Network*, vol. 15, no. 3, pp. 48–53, 2001.
- [9] W. Feng, D. Kandlur, D. Saha, and K. G. Shin, "BLUE: A new class of active queue management algorithms," Tech. Rep. U. Michigan EECS CSE-TR-387-99, 1999.
- [10] W. Feng, D.D. Kandlur, D. Saha, and K.G. Shin, "A self-configuring RED gateway," in *Proceedings of INFOCOM 99*, 1999, pp. 1320–1328.
- [11] S. Floyd, R. Gummadi, and S. Shenker, "Adaptive RED: An algorithm for increasing the robustness of RED," available at <http://www.icir.org/floyd/papers/adaptiveRed.pdf>, Aug. 2001.
- [12] J.S. Jou and J.S. Baras, "A parallel virtual queue structure for active queue management," Tech. Rep. 2003-9, Institute for Systems Research, <http://techreports.isr.umd.edu/ARCHIVE/>, 2003.
- [13] M. Mathis, J. Semke, and Mahdavi, "The microscopic behavior of the TCP congestion avoidance algorithm," *Computer Communication Review*, vol. 27, no. 3, pp. 953–962, 1997.
- [14] D. R. Smart, *Fixed Point Theorems*, Cambridge University Press, London, New York, 1974.
- [15] A. Lasota and M.C. Mackey, *Chaos, Fractals, and Noise: Stochastic Aspects of Dynamics*, Springer-Verlag, second edition, 1994.